

Desulfurization Activity of Ni/NAC Catalysts Prepared by Ultrasonic-Assisted Impregnation

MENG DAN GONG¹, XUE JIAO WANG¹, JIA XIU GUO^{1,2,*}, YONG JUN LIU^{1,2} and HUA QIANG YIN^{1,2,*}

¹College of Architecture and Environment, Sichuan University, Chengdu 610065, Sichuan, P.R. China

²National Engineering Technology Research Center for Flue Gas Desulfurization, Sichuan University, Chengdu 610065, Sichuan, P.R. China

*Corresponding authors: Tel./Fax: +86 28 85403016; E-mail: guojiaxiu@scu.edu.cn; scuarc@163.com

Received: 24 April 2014;

Accepted: 1 July 2014;

Published online: 15 November 2014;

AJC-16323

Nickel-loaded activated carbons treated by HNO₃ (Ni/NAC) were prepared by ultrasonic-assisted impregnation method and characterized by scanning electron microscopy, X-ray diffraction and X-ray photoelectron spectroscopy. Desulfurization activity of catalysts and the effects of different ultrasonic time on desulfurization activity were studied. The results showed that the catalysts prepared by ultrasonic-assisted impregnation exhibit better desulfurization activity compared to the catalysts prepared by a single impregnation. With the increase of the ultrasonic oscillation time, the desulfurization activity increases firstly and then decreases. The catalyst prepared by 80 min ultrasonic oscillation shows the best desulfurization activity and has sulfur capacity of 235.8 mg/g. Nickel and NiO species coexist in all prepared catalysts, but the ultrasonic oscillation can improve the dispersion of the active components and create the chemisorbed oxygen, resulting in the improvement of desulfurization activity of the catalysts.

Keywords: Activated carbon, Ultrasonic oscillation, Desulfurization, Nickel.

INTRODUCTION

Sulfur dioxide is considered as significant atmospheric pollutants not only for its toxicity but also causing acid rain. More efficient desulfurization techniques are desired in SO₂ removal¹. The traditional gas desulfurization technology has many disadvantages, such as secondary pollution and device corrosion. Developing new catalytic flue gas desulfurization technology with low cost, low pollution and high efficiency has become an urgent task. Catalysis is a very effective method for flue gas desulfurization technology. However, the key factor of this technique is to develop an efficient catalyst. The use of activated carbon as supports for desulfurization shows many advantages. Activated carbon (AC) has high specific surface area, abundant pore structure and good acid/base resistance². On the other hand, the surface functional groups on activated carbon act as anchorage sites that interact with the active components improving its dispersion³. Many researchers focus on developing catalysts supported transition metal on activated carbon (AC) for desulfurization, such as CuO/AC⁴ and Fe/AC⁵. In our previous study⁶, it is found that Ni loading on activated carbon can efficiently improve the desulfurization activity of catalysts and the species of active component play an important role in the desulfurization process.

Impregnation is one of the most common catalyst preparation methods, but it has some disadvantages. For example, the loading capacity is low and the active component cannot

disperse uniformly on the support. Many researchers use some supplementary methods to overcome these disadvantages and to achieve a well dispersion of active components, such as ultrasonic oscillation. Bianchi *et al.*⁷ has found that Pd is well dispersed on the carbon supports prepared by ultrasonic-assisted impregnation method. However, the change of metal species and functional groups of activated carbon in the ultrasonic-assisted excessive impregnation were rarely reported before. This study aims to explore the effects of ultrasonic-assisted impregnation on the changes of Ni species and surface functional groups in Ni-supported activated carbon catalysts.

In this study, Ni/AC desulfurization catalysts were prepared by ultrasonic-assisted excessive impregnation method. The effects of ultrasonic oscillation time on the desulfurization activity of catalysts and the active component changes have been investigated by scanning electron microscopy (SEM), X-ray diffraction (XRD) and X-ray photoelectron spectroscopy (XPS).

EXPERIMENTAL

Catalyst preparation: All original activated carbon (Xingtong Chemical Ltd., Henan, China) was crushed into 10-20 mesh and boiled in distilled water for 0.5 h. The obtained activated carbon was washed with distilled water until the washing liquid became neutral and dried for 12 h at 105 °C. The samples were then immersed into HNO₃ (30 vol. %) solution

for 2 h at 60 °C under stirring condition. Subsequently, the samples were filtrated and washed with distilled water until washing fluid became neutral. Finally, the samples were dried in 105 °C for 12 h and denoted as NAC.

Catalysts were prepared by ultrasound-assisted excessive impregnation method. The precursor was $\text{Ni}(\text{NO}_3)_2 \cdot 6\text{H}_2\text{O}$ (AR grade; Kelong Chemical Reagent Factory, Chengdu, China). NAC samples were completely immersed into an appropriate concentration precursor solution to achieve Ni loading of 1 wt. %. During the impregnation, the mixtures were oscillated in an ultrasonic water bath (40 kV) at 40 °C. The samples were oscillated for 0, 20, 40, 60, 80, 100 and 120 min, respectively and kept statically for 12 h. The solution was heated at 60 °C and constantly stirred until the liquid was completely eliminated. Finally, all samples were dried at 105 °C for 12 h, they were calcined at 800 °C for 2 h in a sealed oven under high-purity nitrogen (99.99 %) atmosphere. The heating rate was 5 °C/min. The obtained catalysts were labeled as Ni/NAC-x. x is defined as oscillation time. Thus, the prepared catalysts were named as Ni/NAC-0, Ni/NAC-20, Ni/NAC-40, Ni/NAC-60, Ni/NAC-80, Ni/NAC-100 and Ni/NAC-120, respectively.

Evaluation of catalyst activity: Sulfur dioxide was removed at 80 °C in a fixed bed flow micro-reactor (i.d. 18 mm) containing 15 cm catalysts by passing a flue gas mixture. Gases were controlled by a rotor flow-meter before entering blender. The simulated flue gas contained 0.23 vol. % SO_2 , 10 vol. % O_2 , 10 vol. % water vapor and N_2 as a balance gas. The space velocity (SV) was 800 h^{-1} . The flue gas before and after reactor passed through a H_2O_2 solution (3 %) and formed H_2SO_4 was determined by titrating with NaOH (0.01 mol/L) solution, using bromocresol green and methyl red as an indicator to determine the end point. When SO_2 concentration in the outlet reached to 100 mg/m^3 , it could be considered that the catalyst bed had been penetrated. The corresponding cumulative working time is regarded as the breakthrough time and the cumulative amount of SO_2 removal per unit mass of catalyst is the breakthrough sulfur capacity.

Catalyst characterization: The surface morphology of samples was observed by scanning electron microscopy (SEM) using a JSM-7500F electron microscope (JEOL Co., Japan) at 5 kV. X-ray diffraction (XRD) was used to determine the structural parameters with a DX-2007 diffractometer (Haoyuan

instrument co., Ltd., Dandong Liaoning, China) using $\text{CuK}\alpha$ radiation ($\lambda = 0.15418 \text{ nm}$) at 40 kV and 30 mA. The XRD data were recorded for 2θ values between 10° and 70° with a step size of 0.03. The crystalline phases were identified by comparison with the reference data from the International Center for Diffraction Data (JCPDs). X-ray photoelectron spectroscopy (XPS) was carried out on an XSAM-800 spectrometer (KRATOS Co., UK) with $\text{Al K}\alpha$ radiation under ultra-high vacuum (UHV) at 12 kV and 15 mA. Energy calibration was done by recording the core level spectra of $\text{Au } 4f_{7/2}$ (84.00 eV) and $\text{Ag } 3d_{5/2}$ (368.30 eV). Peak areas including satellites, were computed by a program which assumed Gaussian-line shapes and flat background subtraction.

RESULTS AND DISCUSSION

Desulfurization performance of Ni/NAC catalysts: The curves of the relation between SO_2 removal and working time of NAC and Ni/NAC-x catalysts (a) and the corresponding sulfur capacity (b) are shown in Fig. 1. All Ni/NAC-x exhibit good desulfurization activity and high breakthrough sulfur capacity compared to NAC, indicating that metal mixtures or metal oxides on activated carbon can significantly improve desulfurization performance. This is probably related to the catalytic activity of metal species (active site) during the SO_2 oxidation process. As shown in Fig. 1, the SO_2 removal efficiency of catalysts gradually decreases with time prolonging, revealing that the catalyst is a gradual deactivation process. This may be that SO_2 molecules are firstly adsorbed on the active sites of catalysts and then oxidized to SO_3 , followed by hydration to form H_2SO_4 with H_2O in the simulated flue gas¹. The generated H_2SO_4 may occupy the active site, resulting in the decrease of desulfurization activity. At the same time, it is found that the ultrasonic oscillation time significantly influence the desulfurization activity of Ni/NAC-x. The breakthrough sulfur capacity and breakthrough time of Ni/NAC-0 are 132 mg/g and 463 min, respectively. With the increase of the ultrasonic oscillation time, the desulfurization activity increases firstly and then decreases. When the oscillation time is 80 min, the Ni/NAC-80 exhibits the best desulfurization activity. It can keep 100 % desulfurization efficiency for 800 min and the corresponding sulfur capacity is 236 mg/g. When

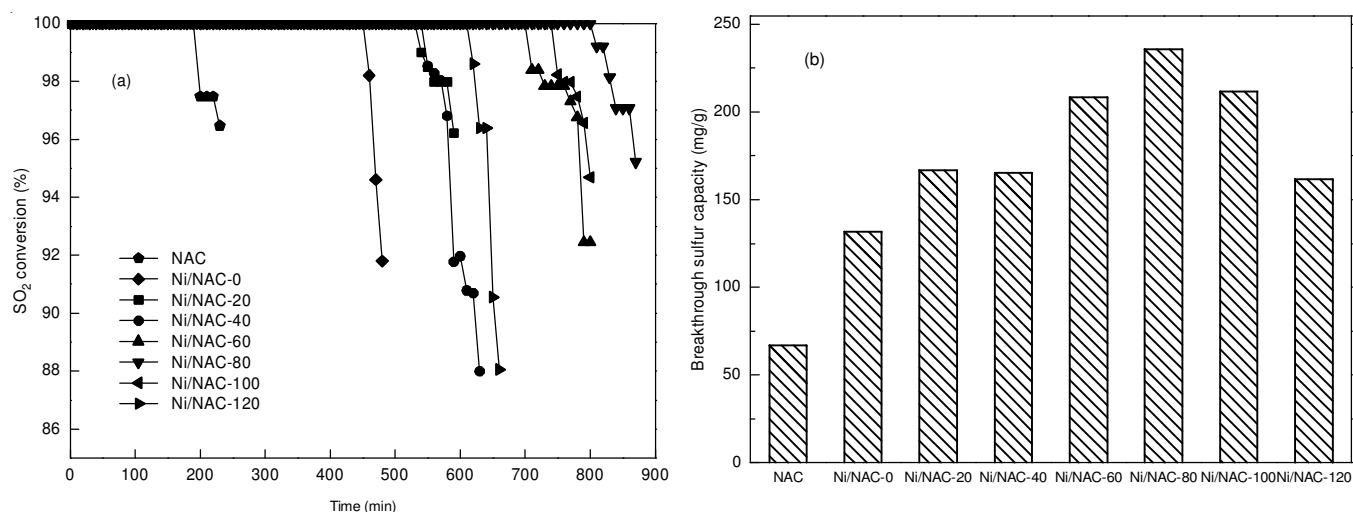


Fig. 1. Desulfurization working curves of NAC and Ni/NAC-x (a) and their breakthrough sulfur capacity (b)

oscillation time is more than 80 min, the sulfur capacity of catalyst decreases and the breakthrough time shortens to a certain extent. This indicates that oscillation time of 80 min is optimum in our experiments. The main reason of this case could be that the surface physical structure of activated carbon changes under the long time oscillation. The ultrasound produces cavitation effect under the high energy situation and forms the internal jet with strong impact force. The internal jet can accelerate the diffusion rate of the loading and improve the dispersion of active components. Thus, the catalyst can provide more active sites to adsorb and transform the SO_2 from the flue gas⁷⁻¹⁰. On the other hand, if the oscillation time is too long, the energy will be too high, leading to the devastation of activated carbon structure and the collapse of pore structure¹¹. They are not conducive to the anchor and dispersion of the active ingredients, resulting in the decrease of desulfurization activity.

SEM: SEM patterns of selected samples are illustrated in Fig. 2 to study the effects of ultrasonic oscillations on the surface morphology of catalysts. For Ni/NAC-0, many white crystalline particles are gathered on the surface of activated carbon with an abundant pore structure, which may include catalytic components and some impurities, indicating that the active ingredient can be dispersed on the surface of supports *via* impregnation method. After the ultrasonic assistance is introduced, the surface of selected samples takes place changes. This is mostly caused by the cavitation effect which is created by the synergic effect of ultrasound shock waves. For Ni/NAC-20, the white crystalline particles become small and are uniformly dispersed on the surface of activated carbon and activated carbon still has a well-developed pore structure. These are main reasons for improving the desulfurization activity of Ni/NAC-20. The results are in agreement with the literatures^{9,12}. When the oscillation time increases to 80 min, the white crystalline particles on Ni/NAC-80 become smaller and are more uniformly dispersed on the surface of activated carbon. At the same time, the pore structure is not destroyed by ultrasound but become smoother than other samples. The reason may be that the cavitation effect caused by ultrasonic

oscillation which can remove the slight impurities from the support surface, leading to form more active sites^{13,14} and has high catalyst activity. When the oscillation time increases to 120 min, the white crystalline particles on Ni/NAC-120 become scarce and pore structures of activated carbon are destroyed. This may be that the ultrasonic wave with high energy plays mainly wash role and the active ingredient could be washed off, resulting in less active sites and the decrease of desulfurization activity.

Surface chemical properties of catalysts before desulfurization: The XRD patterns of selected samples before desulfurization are shown in Fig. 3. The selected samples exhibit wide dispersion peaks around $20\text{--}30^\circ$ and $30\text{--}40^\circ$ in 2θ range, which is assigned to the characteristic peaks of graphite structure of activated carbon, showing that the ultrasonic oscillation does not destroy carbon supports in preparation process. The obvious peaks at $2\theta = 20.86^\circ$, 26.56° and 36.43° observed on the broad carbon peaks are identified as silica (JCPDs 46-1045). The diffraction peak at 35.20° is assigned to calcium compounds (JCPDs 15-0012) which come from the original activated carbon. For Ni/NAC-0, distinct diffraction peaks at $2\theta = 44.5^\circ$ and 51.8° are due to Ni (JCPDS 04-0850) which are corresponding to (111) and (200) plane and small characteristic peak of NiO at $2\theta = 43.29^\circ$ (JCPDs 78-0643) is observed, indicating that Ni and NiO coexist in catalysts. After the ultrasonic assistance is introduced, the diffraction peaks of Ni at $2\theta = 44.3^\circ$ and 51.6° are observed, but the diffraction peaks of NiO are not clearly detected. This could be due to a high dispersion of NiO, or diffraction peaks of NiO are too weak to be masked by some impurity peaks and noise. Comparison with the XRD patterns of Ni/NAC-0 catalysts, the diffraction peaks of Ni in Ni/NAC-20 catalysts become diffuse and broad, implying that Ni on activated carbon is more dispersed, which is due to the cavitation effect of ultrasonic oscillation. Furthermore, the characteristic peaks of Ni for the Ni/NAC-20 slightly shift to a lower angle of (111) and (200) plane. The phenomenon is attributed to the lattice swelling of Ni¹⁵. The interplanar spacing of Ni may expand with the decrease of grain size which caused by ultrasonic oscillation and the expansion of Ni leads to the improvement of lattice defect¹⁶. This lattice

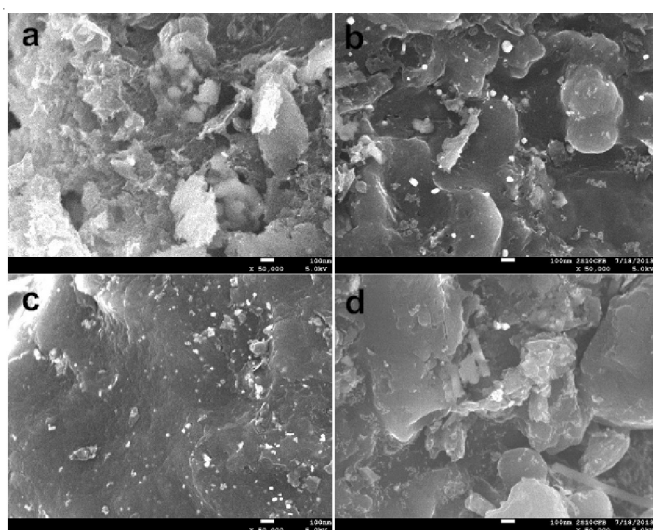


Fig. 2. SEM images of the catalysts, (a) Ni/NAC-0; (b) Ni/NAC-20; (c) Ni/NAC-80; (d) Ni/NAC-120

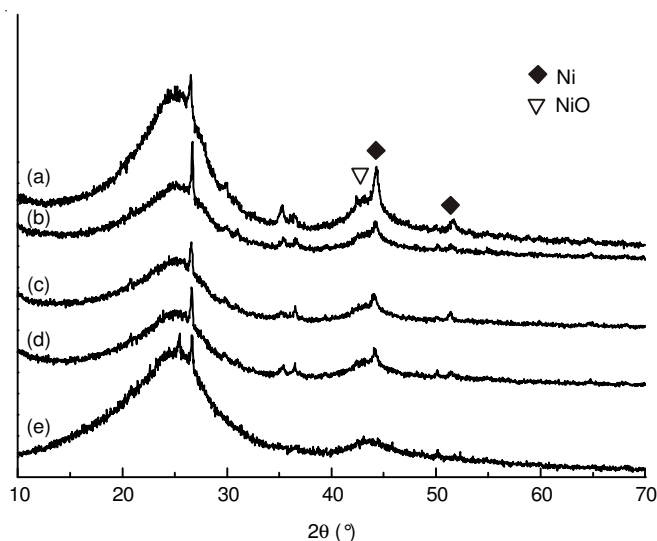


Fig. 3. XRD patterns of the samples, (a) Ni/NAC-0; (b) Ni/NAC-20; (c) Ni/NAC-80; (d) Ni/NAC-120; (e) Ni/NAC-80 after desulfurization

defect is beneficial to the gas adsorption¹⁷. This is another reason that the catalysts prepared by ultrasonic assistance have better desulfurization activity. For Ni/NAC-80 and Ni/NAC-120, characteristic peaks of Ni at $2\theta = 44.1^\circ$ and 51.4° are still observed. The former is more diffuse, showing a high dispersion and the latter becomes a bit sharp, indicating an aggregation of active components and poor dispersion, which is proved in SEM. This indicates that the oscillation time is too long not to help the dispersion of the active ingredient but to make them gather, resulting in the decrease of desulfurization activity.

The Ni $2p$ XPS spectra of Ni/NAC-0 and Ni/NAC-80 before desulfurization are shown in Fig. 4 to further clarify catalytic active species of the metal additives in activated carbon. Generally, the main peaks around 854.50–855.16 eV with satellite peaks at 860.98–861.56 eV are attributed to the spin-orbit split lines of Ni $2p_{3/2}$ and the ranges at 872.03–873.20 eV with satellite peaks at 878.39–879.97 eV correspond to the spin-orbit split lines of Ni $2p_{1/2}$. The Ni $2p_{3/2}$ binding energies of 853.9–854.9 eV and the shake-up satellite peak at 860.8–862.8 eV are assigned to NiO^{19,20} and the Ni $2p_{3/2}$ binding energy of Ni⁰ appears at 852.7 eV²¹. For Ni/NAC-0, the Ni $2p_{3/2}$ binding energies at 854.50 and 860.98 eV and the Ni $2p_{1/2}$ binding energies at 872.03 and 878.91 eV are attributed to NiO, which is in agreement with the reference^{22,23}. For Ni/NAC-80, the Ni $2p_{3/2}$ binding energies at 854.82 and 861.25 eV and the Ni $2p_{1/2}$ binding energies at 872.57 and 879.33 eV are also attributed to NiO, indicating that NiO has been generated in Ni/NAC-80. There are no obvious peaks of Ni species. The most probable reason is that the XPS is a surface technique and then only gives an estimative of the chemical composition of the uppermost surface layers (about 10–15 nm in depth)²⁴. The Ni on the surface could be oxidized to NiO when it is exposed to the air. Another potential reason may be that the change of morphology is induced by the oscillation effect²⁵. Based on the results of XRD and XPS, it can be concluded that the Ni and NiO coexist in activated carbon and the state of active components has not been changed by the ultrasonic oscillation. The coexistence of Ni and NiO in the catalysts is conducive to the SO₂ removal⁶. According to the metal oxide catalytic mechanism, the oxidative reactions firstly utilize lattice oxygen and the lattice oxygen is replenished from the gas phase oxygen. In our experiment, the SO₂ is oxidized to SO₃ which will firstly utilize lattice oxygen from NiO on the catalysts; Ni⁰ is oxidized to NiO by the gas phase oxygen. In Fig. 3a and c, the diffraction peak of Ni⁰ in Ni/NAC-0 is a little sharp and the intensity is higher than Ni/NAC-80, which is due to the decrease of the crystallite size of Ni species in Ni/NAC-80²⁶. The results of SEM also prove that the active components are well dispersed on activated carbon. That's to say that the ultrasonic wave can improve the dispersion of active component on the supports, leading to the enhancement of the desulfurization activity of Ni/NAC-80.

The C 1s and O 1s XPS patterns of selected samples before desulfurization are shown in Fig. 5 to investigate the influence of ultrasonic wave on the surface functional groups. The C 1s XPS spectra of Ni/NAC-0 and Ni/NAC-80 are similar but the O 1s peaks take place changes. The C 1s peaks of two samples are deconvoluted into four peaks, including graphite carbon

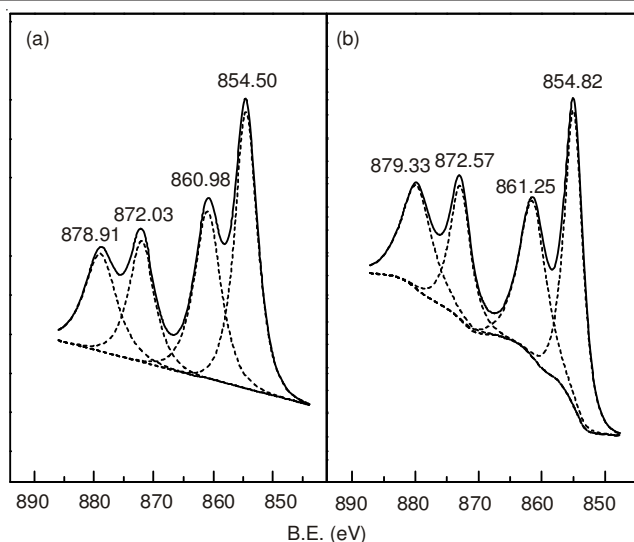


Fig. 4. Ni $2p$ XPS spectra of Ni/NAC-0 (a) and Ni/NAC-80 (b)

(BE = 284.73 and 284.65 eV), carbon species in alcohol and/or ether groups (BE = 286.36 and 285.65 eV), carbon in carbonyl group (BE = 287.69 and 287.32 eV), carboxyl and/or ester groups (BE = 290.07 and 289.87 eV) respectively^{27,28}. In Fig. 5a and b, it is found that the relative content of different functional groups changes a little after ultrasonic oscillation. The increase of the relative content of C=O on Ni/NAC-80 play a favorable role in their improved SO₂ adsorption performance because C=O is the active center for SO₂ oxidation²⁹. For Ni/NAC-0, the O 1s peaks at 529.60, 532.17 and 533.55 eV are attributed to NiO³⁰, C=O^{5,31} and absorbed water³², respectively. For Ni/NAC-80, the O 1s peaks at 529.59, 531.32, 532.99 and 534.35 eV are assigned to NiO³⁰, C=O and/or O=C-OH^{5,31}, -O- and/or -OH^{5,31} and chemisorbed oxygen^{31,33}, respectively, showing that the active component NiO doesn't change but the chemisorbed oxygen appears after ultrasonic assistance. This chemisorbed oxygen is very important because NiO species can transfer electrons to adsorbed molecule oxygen, resulting in formation³⁴ of O²⁻. The presence of oxygen species in the catalysts is directly related to the oxidation reaction in the multi-phase, because this involves reactive oxygen species. The "ionic" oxygen is active in total oxidation, which can improve SO₂ oxidation.

Surface chemical properties of catalysts after desulfurization: The Ni $2p$ XPS spectra of Ni/NAC-80 after desulfurization are shown in Fig. 6 a. The Ni $2p_{3/2}$ binding energies at 854.99 and 861.41 eV and the Ni $2p_{1/2}$ binding energies at 872.87 and 879.74 eV are attributed to Ni₂O₃⁶, indicating that the active components Ni and NiO are transformed into Ni₂O₃ in SO₂ removal process. In Fig. 3e, the diffraction peaks of Ni and NiO disappear after desulfurization, indicating that the active components take place changes after desulfurization. This is the most important reason for the catalyst deactivation. Compared with the samples before desulfurization, many diffraction peaks disappear, implying that most impurities are eliminated during the desulfurization because many impurities can be dissolved by the generated H₂SO₄.

The C 1s, O 1s and S $2p_{3/2}$ XPS spectra of Ni/NAC-80 after desulfurization are shown in Fig. 6 b, c and d. The C 1s binding energies don't change significantly compared to the fresh

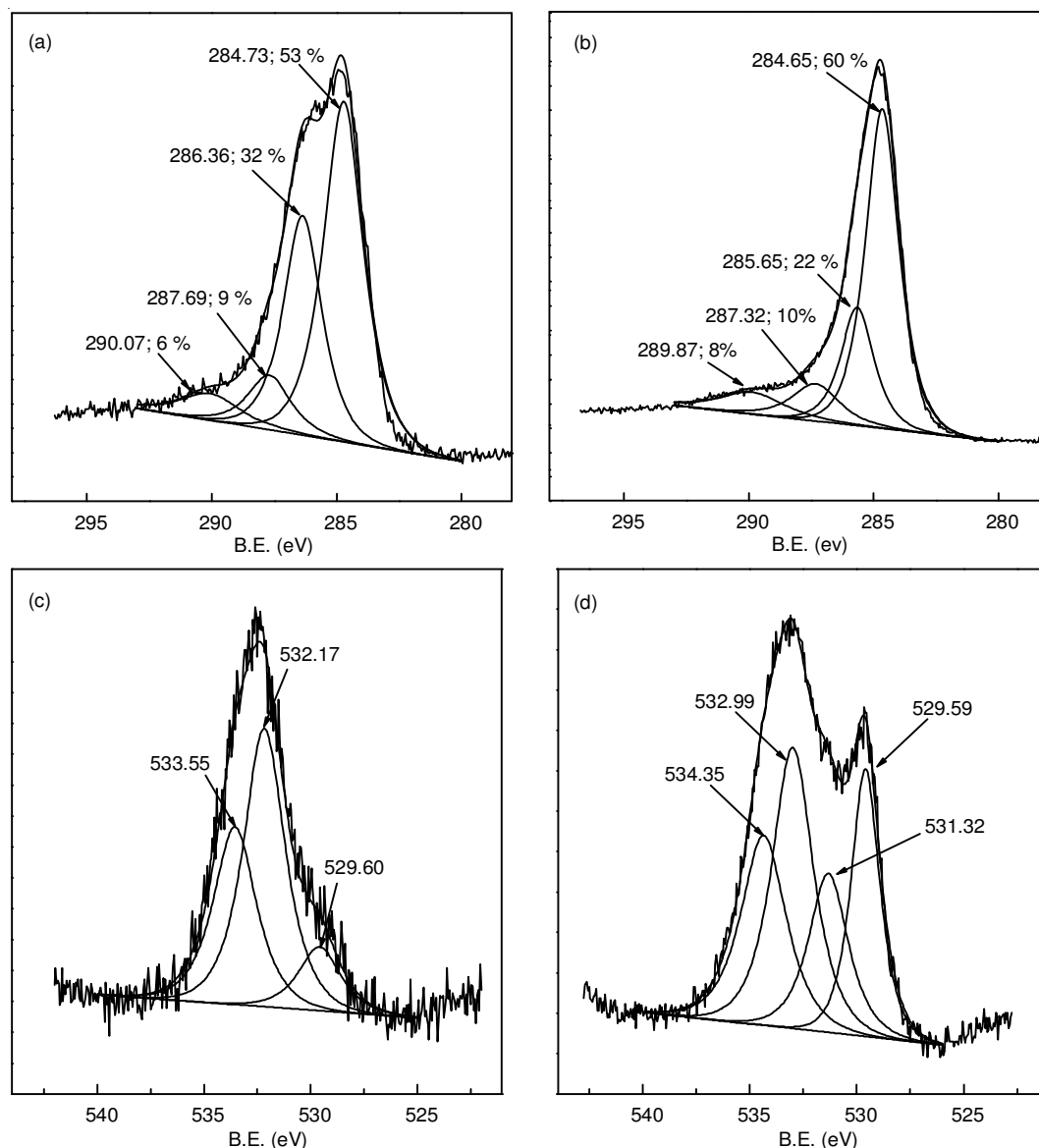


Fig. 5. C 1s and O 1s XPS spectra of Ni/NAC-0 (a) and (c) and Ni/NAC-80 (b) and (d)

samples. The binding energies at 284.69, 285.77, 287.10 and 289.32 eV are attributed to the C-C, C-OH and/or C-O-C, C=O, O=C-OH and/or O=C-O-C, respectively^{27,28}. The relative content of C-OH and/or C-O-C, C=O, O=C-OH and/or O=C-O-C are 17, 8 and 6 %, indicating that the amount of oxygen-containing functional groups decrease compared to the Ni/NAC-80 before desulfurization. The content of carbonyl groups decreases after desulfurization, which is a factor for the inactivation²⁹. The distinct peaks for O 1s at 529.91, 532.07 and 533.19 eV are associated with Ni₂O₃, C=O and H₂O³², indicating that surface oxygen species of catalysts after desulfurization takes place changes, especially the disappearance of NiO and chemisorbed oxygen, resulting in the deactivation of catalysts.

The S 2p_{3/2} binding energy at 169.57 eV is assigned to S⁶⁺ of SO₄²⁻, indicating that the S mainly exists as SO₄²⁻ on Ni/NAC-80 after desulfurization²⁹. Combined with the Ni 2p XPS spectra and XRD of Ni/NAC-80 after desulfurization, no NiSO₄ is observed, proving that the SO₂ in simulated flue gas is oxidized to SO₄²⁻ by the catalyst and the SO₄²⁻ hydrates with water

and forms H₂SO₄. The generated H₂SO₄ existed in the pore structure of activated carbon and covered active sites, resulting in the deactivation of catalysts.

Conclusion

Ultrasonic oscillation can enhance the desulfurization activity of Ni/NAC catalysts. The appropriate ultrasonic assistance does not destroy the structure of activated carbon or change the active component state but can create the chemisorbed oxygen and improve the dispersion of the active component on support, resulting in the improvement of the desulfurization activity. Ultrasonic oscillation is a useful supplementary method to prepare the high-efficiency desulfurization catalyst and oscillation time is a key factor in affecting the desulfurization performance.

ACKNOWLEDGEMENTS

This work is financially supported by the National Nature Science Youth Fund of China (No.5110828) and the Sichuan Provincial Science and Technology Agency Public Research

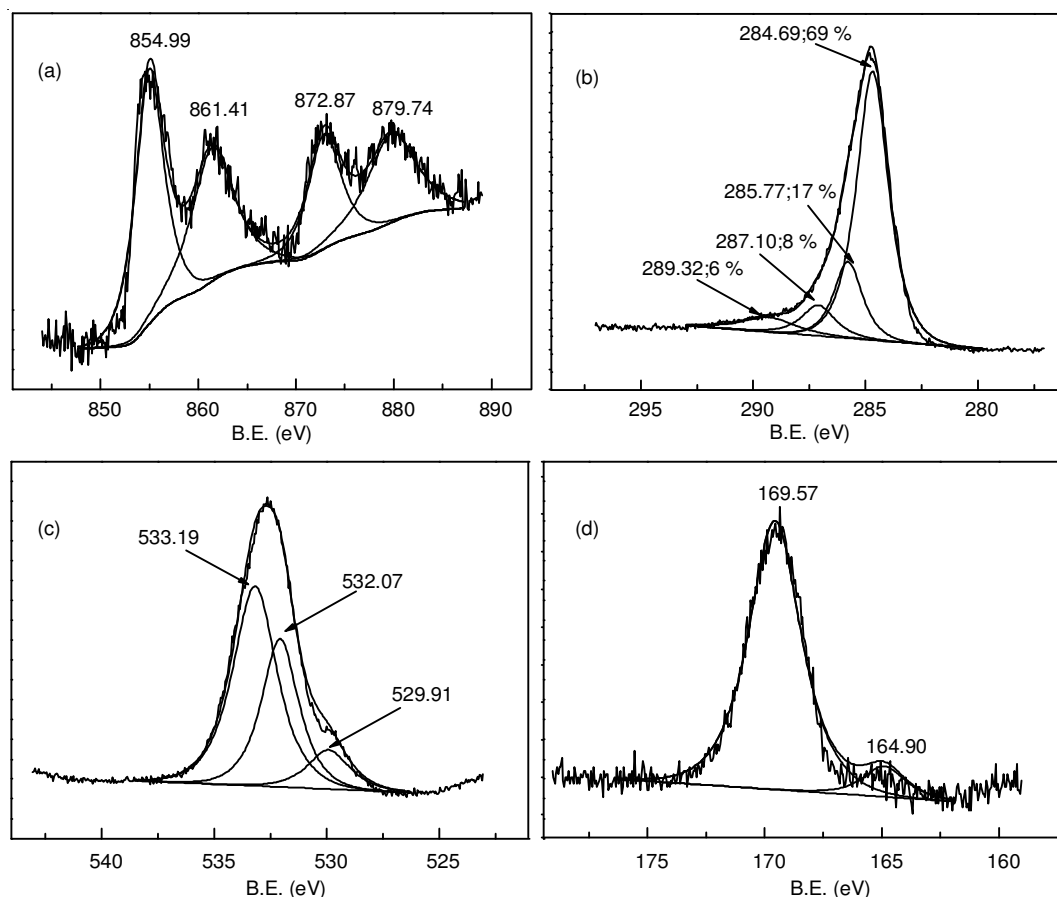


Fig. 6. XPS spectra of Ni/NAC-80 after desulfurization: (a) Ni 2p, (b) C 1s, (c) O 1s and (d) S 2p_{3/2}

Projects (No.2012GZX0028). We would like to thank the Analytical & Testing Center of Sichuan University for the SEM characterization of the catalysts.

REFERENCES

1. Z. Yan, J. Wang, R. Zou, L. Liu, Z. Zhang and X. Wang, *Energy Fuels*, **26**, 5879 (2012).
2. H.H. Tseng and M.Y. Wey, *Chemosphere*, **62**, 756 (2006).
3. A. Gil, G. Puente and P. Grange, *Micropor. Mater.*, **12**, 51 (1997).
4. P. Gao and X.L. Ma, *Central China Electric Power*, **18**, 1 (2005).
5. X.-L. Liu, J.-X. Guo, Y.-H. Chu, D.-M. Luo, H.-Q. Yin, M.-C. Sun and R. Yavuz, *Fuel*, **123**, 93 (2014).
6. J.X. Guo, J. Liang, Y.H. Chu, H.Q. Yin and Y.Q. Chen, *Chin. J. Catal.*, **31**, 278 (2010).
7. C.L. Bianchi, E. Gotti, L. Toscano and V. Ragaini, *Ultrason. Sonochem.*, **4**, 317 (1997).
8. K. Matsuyama and K. Mishima, *Ind. Eng. Chem. Res.*, **49**, 1289 (2010).
9. J. Guo, Y.J. Hou, C. Yang, Y. Wang and L. Wang, *Mater. Lett.*, **67**, 151 (2012).
10. K. Sato, J.G. Li, H. Kamiya and T. Ishigaki, *J. Am. Ceram. Soc.*, **91**, 2481 (2008).
11. F.W. Yu, J.B. Ji, C. Huo, W.F. Han, X.N. Li and H.Z. Liu, *Chin. J. Catal.*, **26**, 485 (2005).
12. C. Sauter, M.A. Emin, H.P. Schuchmann and S. Tavman, *Ultrason. Sonochem.*, **15**, 517 (2008).
13. F. Yu, J. Ji, Z. Xu and H. Liu, *Ultrasonics*, **44**, 389 (2006).
14. H. Li, J. Zhang and H.X. Li, *Catal. Commun.*, **8**, 2212 (2007).
15. T. Sawabe, M. Akiyoshi, K. Yoshida and T. Yano, *J. Nucl. Mater.*, **417**, 430 (2011).
16. Z.Q. Wei, T.D. Xia, J. Ma, W.J. Feng, J.F. Dai, Q. Wang and P.X. Yan, *Mater. Charact.*, **58**, 1019 (2007).
17. A.M. Mazzone and V. Morandi, *Appl. Surf. Sci.*, **253**, 4010 (2007).
18. Y. Liu, Y.X. Yu and W.D. Zhang, *Electrochim. Acta*, **59**, 121 (2012).
19. A.A. Lemonidou, M.A. Goula and I.A. Vasalos, *Catal. Today*, **46**, 175 (1998).
20. N.S. McIntyre and M.G. Cook, *Anal. Chem.*, **47**, 2208 (1975).
21. Z. Song, X. Bao, U. Wild, M. Muhler and G. Ertl, *Appl. Surf. Sci.*, **134**, 31 (1998).
22. C. Lee and R. Doong, *Environ. Sci. Technol.*, **42**, 4752 (2008).
23. H.W. Kim, K.M. Kang and H.Y. Kwak, *Int. J. Hydrogen Energy*, **34**, 3351 (2009).
24. O.S.G.P. Soares, J.J.M. Órfão, J. Ruiz-Martínez, J. Silvestre-Albero, A. Sepúlveda-Escribano and M.F.R. Pereira, *Chem. Eng. J.*, **165**, 78 (2010).
25. Y.B. Tu, J.Y. Luo, M. Meng, G. Wang and J.J. He, *Int. J. Hydrogen Energy*, **34**, 3743 (2009).
26. Y.A. Ryndin, L.V. Nosova, A.I. Boronin and A.L. Chuvilin, *Appl. Catal.*, **42**, 131 (1988).
27. S. Biniak, G. Szymanski, J. Siedlewski and A. Swiatkow, *Carbon*, **35**, 1799 (1997).
28. K. László, E. Tombácz and K. Josepovits, *Carbon*, **39**, 1217 (2001).
29. X.S. Zhao, G.Y. Cai, Z.Z. Wang, Q.X. Wang, Y.H. Yang and J.S. Luo, *Appl. Catal. B*, **3**, 229 (1994).
30. N.S. McIntyre and M.G. Cook, *Anal. Chem.*, **47**, 2208 (1975).
31. A.M. Puziy, O.I. Poddubnaya, R.P. Socha, J. Gurgul and M. Wisniewski, *Carbon*, **46**, 2113 (2008).
32. Z. Song, X. Bao, U. Wild, M. Muhler and G. Ertl, *Appl. Surf. Sci.*, **134**, 31 (1998).
33. S.J. Park and W.Y. Jung, *J. Colloid Interf. Sci.*, **250**, 93 (2002).
34. B. Stöhr, H.P. Boehm and R. Schlögl, *Carbon*, **29**, 707 (1991).